J Clust Sci (2013) 24:1151–1162
DOI 10.1007/s10876-013-0605-0

ORIGINAL PAPER

Synthesis, Characterization, Photoluminescence and Photocatalytic Properties of CeO_2 Nanoparticles by the Sonochemical Method

Parastoo Jamshidi · Masoud Salavati-Niasari · Davood Ghanbari · Hamid Reza Shams

Received: 1 November 2012 / Published online: 2 July 2013

Abstract Uniform CeO_2 nanoparticles were synthesized via a facile sonochemical reaction between ceric ammonium nitrate and ammonia. Nanoparticles were synthesized via a surfactant free reaction at room temperature in solvent of water. Products were characterized using X-ray diffraction, scanning electron microscopy, photoluminescence (PL) spectroscopy, and energy dispersive X-ray analysis. The effect of different parameters such as precursor, power of pulsation, surfactant and reaction time on the morphology of the products was investigated. It was found that the as-obtained CeO_2 nanoparticles exhibit a strong PL peak at 381 nm at room temperature that can be ascribed to the high level transition in the CeO_2 semiconductor. The photocatalytic behavior of CeO_2 nanoparticles was evaluated using the degradation of a methyl orange aqueous solution under ultraviolet light irradiation. The results show that CeO_2 nanoparticles are promising materials with excellent performance in photocatalytic applications.

Keywords CeO_2 · Sonochemical method · Nanoparticle

Introduction

Nanometer-sized particles have gained much attention among all of the materials science, because the properties of nanocrystals depend not only on their composition but also on their size, shape, structure, phase and size distribution. Cerium oxide nanoparticles have exceptional luminescence, magnetic and electronic properties due to their unfilled 4f electronic structure. It has been attracting great interest because of its effective technological applications, such as electrochemical devices,

P. Jamshidi · M. Salavati-Niasari (✉) · D. Ghanbari · H. R. Shams
Institute of Nano Science and Nano Technology, University of Kashan,
P.O. Box 87317-51167, Kashan, Islamic Republic of Iran
e-mail: salavati@kashanu.ac.ir

catalysts for three-way automobile exhaust systems, abrasives for chemical–mechanical planarization, ultraviolet absorbents, oxygen storage capacity, hydride solar cell, H_2S removal and luminescent materials [1–5]. Ceria is widely used as an oxygen pumps and amperometric oxygen monitors because of its high oxygen ion conductivity. Ceria has also received much success in redox and combustion catalysts due to its ability to shift between reduced and oxidized state as a result of change in gas phase oxygen concentration. There are several methods employed for the preparation of cerium oxide such as precipitation, sonochemical, solvothermal, microemulsion, mechanochemical, thermal decomposition, spray pyrolysis and sol–gel method [6–10]. Sonochemical method is a facile route operated under ambient conditions [11, 12]. During sonication, ultrasonic waves radiate through the solution causing alternating high and low pressure in the liquid media. It has been well recognized that ultrasonic irradiation caused cavitation in a liquid medium where the formation, growth and implosive collapse of bubbles occurred. The collapse of bubbles with short lifetimes produces intense local heating and high pressure. These localized hot spots can generate a temperature of around 5,000 °C and a pressure of over 1,800 kPa that these spots are appropriate for many chemical reactions [13, 14]. In this work, we report a room temperature synthesis of CeO_2 nanoparticles using sonochemical reaction. Particles were achieved by employing a sonochemical method, and using different surfactant to control morphology and particle size. Methyl orange (MeO: a typical organic pollutant) was employed as a target because of the relative stability of its molecular structure. The as-prepared nanoparticles have the potential to be applied to ameliorate environmental problems associated with organic and toxic water pollutants.

Experimental

Materials and Methods

Ceric ammonium nitrate $(NH_4)_2Ce(NO_3)_6$, ammonia (32 %), cetyltrimethylammonium bromide (CTAB), sodium dodecanesulfonate (SDS: 99 %), polyethylene glycol (PEG600, 1L = 1.3 kg), poly vinyl pyrrolidone were purchased from Merck Company. PVP-K40-$(C_6H_9NO)n$ $(n = 40)$ 99 % purity, was purchased from Sigma-Aldrich. All of the chemicals were used as received without further purifications. XRD patterns were recorded by a Philips, X-ray diffractometer using Ni-filtered Cu Kα radiation. A multiwave ultrasonic generator (Sonicator 3000; Bandeline, MS 72, Germany), equipped with a converter/transducer and titanium oscillator (horn), 1.25×10^{-2} m in diameter, surface area of ultrasound irradiating face: 1.23×10^{-4} m^2, operating at 20 kHz, was used for the ultrasonic irradiation and the horn was operated at 50 % amplitude. All ultrasonication experiments were carried out at ultrasonic power between 84 and 125 mW measured by calorimetry [15]. SEM images were obtained using a Hitachi instrument model S4160. Energy dispersive X-ray (EDX) analyzer for elemental analysis was obtained using an Oxford instrument. Prior to taking images, the samples were coated by a very thin layer of Pt to make the sample surface conductor and prevent charge accumulation,

Table 1 Intensity and actual power of three different used conditions

Power (W)	Intensity (W/m^2)	Actual power (mW)
45	1.8×10^5	84
60	2.4×10^5	109
75	3.0×10^5	125

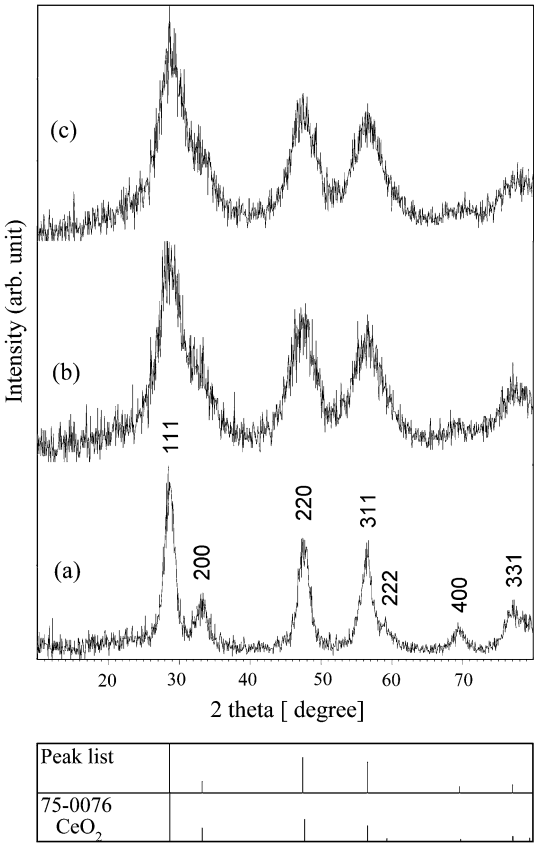

Fig.. 1 XRD pattern of the CeO_2 nanoparticles synthesized **a** without surfactant, **b** by CTAB and **c** by SDS

and obtaining a better contrast. Room temperature photoluminescence was studied by a Perkin Elmer fluorescence instrument.

Synthesis of CeO_2 Nanoparticles

First 0.2 g of ceric ammonium nitrate is dissolved in 100 mL of distilled water. Then 10 mL of NH_3 32 % is added 1 mL/min to the solution, under ultrasonic waves (45, 60 or 75 W that actual power for these values are 84, 109 or 125 mW respectively) for 30 min (Table 1). A yellow precipitate is obtained confirming the synthesis of CeO_2. The precipitate of CeO_2 is then centrifuged and rinsed with

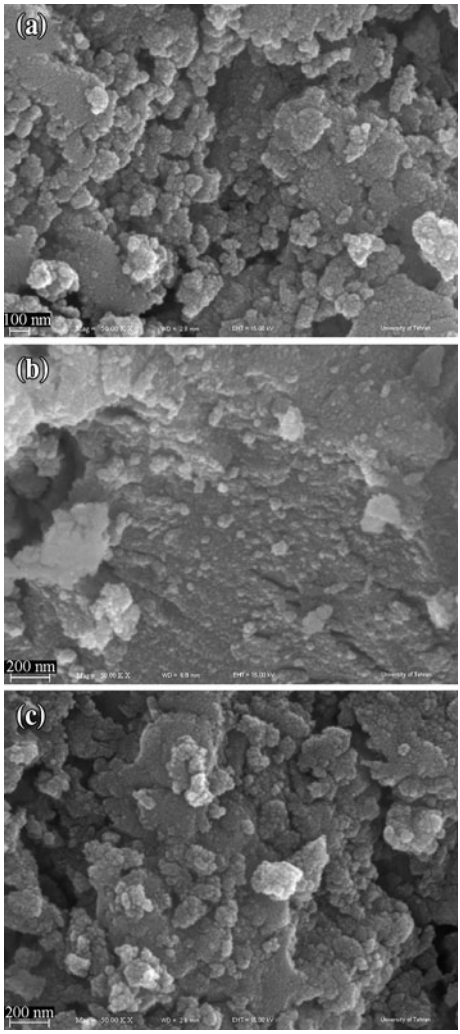

Fig. 2 SEM images of the CeO_2 prepared at 30 min at different power **a** 45 W, **b** 60 W and **c** 75 W

distilled water, followed by being left in room temperature to dry off. (1 mol $(NH_4)_2Ce(NO_3)_6$: 1 mol CeO_2, theoretical yield of CeO_2: 0.62 g, actual yield: 0.56 g).

Results and Discussion

The XRD patterns of CeO_2 nanoparticles obtained without surfactant, with CTAB and SDS are shown in Fig. 1a–c respectively. The patterns is indexed as a cubic phase (space group: *Fm*-3*m*) which is very close to the literature values (JCPDS No. 75-0076), the narrow sharp peaks indicate that the CeO_2 nanoparticles are well

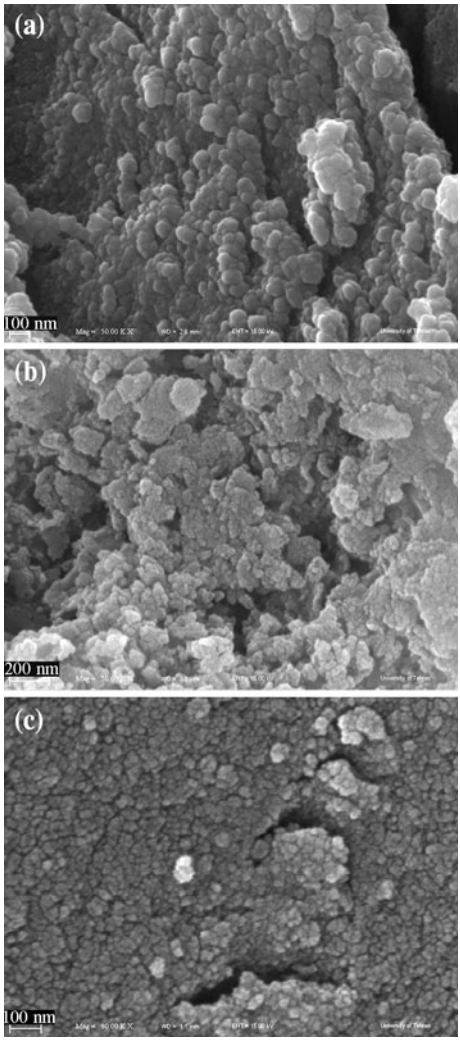

Fig. 3 Obtained products at 45 W (30 min) with different surfactants **a** CTAB, **b** SDS and **c** PVP

crystallized. As Fig. 1a shows by using surfactants the obtained patterns show lower crystallinity related to the pure product.

The crystallite size measurements were also carried out using the Scherrer equation

$$Dc = 0.9\lambda/\beta\cos\theta$$

where β is the breadth of the observed diffraction line at its half intensity maximum, and λ is the wavelength of X-ray source used in XRD. The estimated crystallite size of the samples prepared without surfactant, with CTAB and SDS are 7, 5 and 5 nm respectively.

Ultrasonic irradiation creates bubbles which produces high temperature and energy after decomposition. This process provides appropriates amounts of energy

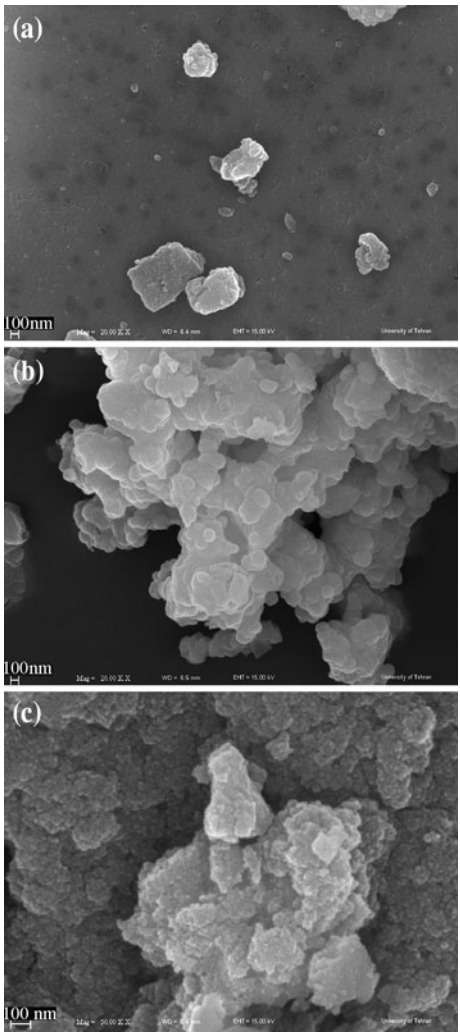

Fig. 4 SEM images of synthesized products at 60 W (30 min) with **a** CTAB, **b** SDS and **c** PVP

for formation of CeO_2 nanoparticles. SEM images of the CeO_2 prepared at 30 min at different powers (45, 60 or 75 W that actual powers for these values are 84, 109 or 125 mW respectively) are shown in Fig. 2a–c respectively. Room temperature synthesis of CeO_2 at 60 W at reaction time of 30 min (Fig. 2a) has been selected as a basic reaction in this work and the effect of change of different parameters on the morphology of the products has been investigated.

Figure 2a depicts nanoparticles with average diameter of 60 nm which are synthesized by increasing the power from 60 to 75 W smaller nanoparticles were obtained. At 60 W growth occurs more than nucleation and bigger particles will be achieved.

It was found that the sonochemical reactions occur within the interfacial region, forming nanocrystals due to the very high quenching rate experienced by the

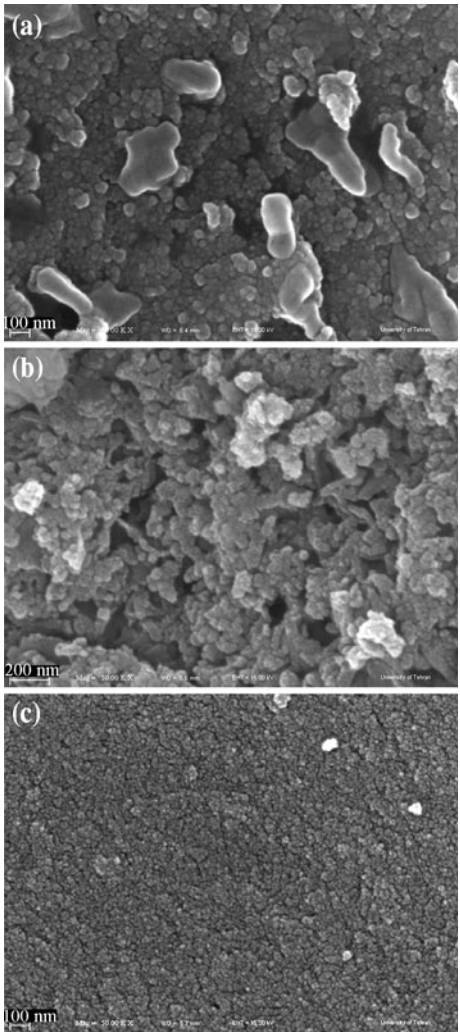

Fig. 5 SEM images of achieved products at 75 W (30 min) with **a** CTAB, **b** SDS and **c** PVP

products. Some parameters influence on cavitation such as low vapor pressure, high surface tension and high sound speed.

The impact of surfactant on the morphology of the CeO_2 which is synthesized at 45 W (30 min) with CTAB, SDS and PVP are shown in Fig. 3a–c respectively. In all of three different conditions nanoparticles are synthesized and by using PVP smallest size are obtained, it can be referred to form non-charge intermediate.

The effect of power of pulsation on the morphology of the CeO_2 is shown in Figs. 4 and 5. SEM images of CeO_2 synthesized at 60 W (30 min) with CTAB, SDS and PVP are shown in Fig. 4a–c respectively.

Figure 4a shows SEM image of bulk product obtained by using CTAB and Fig. 4b illustrates SEM image of CeO_2 synthesized by SDS. SEM image of nanoparticles achieved by PVP is shown in Fig. 4c.

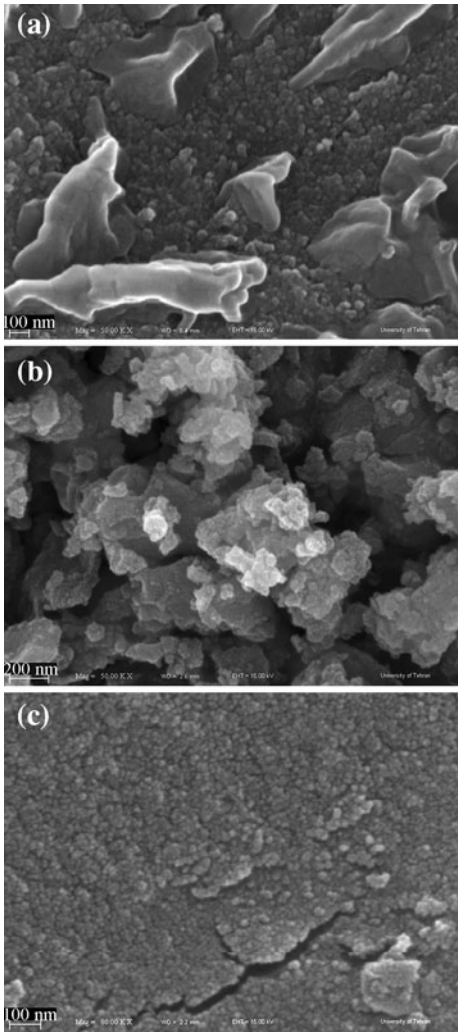

Fig. 6 As synthesized products at 60 W (45 min) with **a** CTAB, **b** SDS and **c** PVP

SEM images of CeO_2 which is synthesized at 75 W (30 min) with CTAB, SDS and PVP are shown in Fig. 5a–c respectively. As it is obvious from the figures, nanoparticles are synthesized and by using PVP agglomerated and smaller nanoparticles are obtained. These results indicate that sonication is favorable to produce CeO_2 nanoparticles with uniform shape. With application of ultrasound irradiation, the formed bubbles collapse, resulting in the generation of high speed microjets with very high velocity which can generate CeO_2 nanoparticles [13].

During the ultrasound cycles, the cavitation bubbles will collapse, forming micro-jets that instantaneously generate intense local heating and high pressure. The micro-jet impact can develop pressures of about 2×10^8 Pa, and a local heating and cooling rate above 10^9 K/s. In fact, cavitation damage is generated by the non-spherical symmetric collapse of a cavitation bubble, either at or near a solid surface.

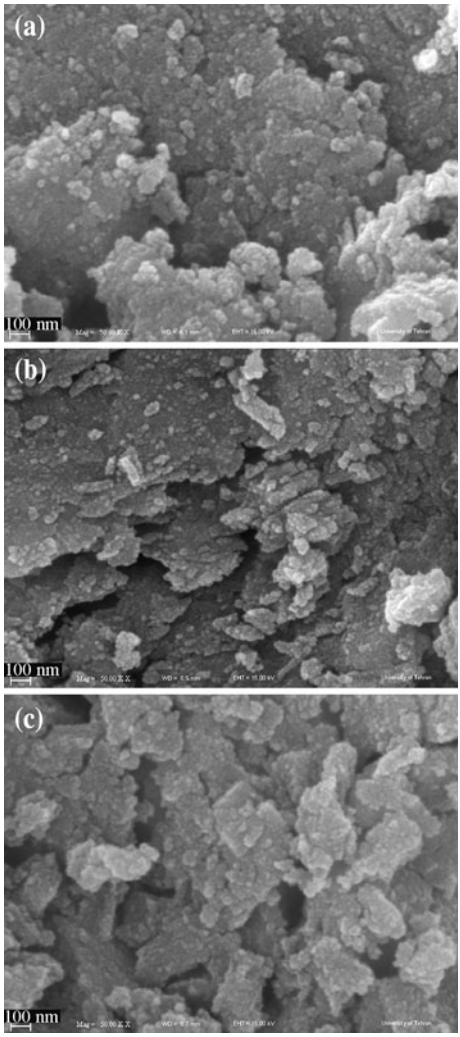

Fig. 7 Obtained products at 60 W (30 min) in propylene glycol with **a** CTAB, **b** SDS and **c** PVP

Violent collapse of bubbles in asymmetrical geometries occur in a number of situations of practical interest including cavitation, shock-wave and laser lithotripsy [14–18].

Reaction time effect on the morphology of the CeO_2 which is synthesized at 45 min (60 W) with CTAB, SDS and PVP are illustrated in Fig. 6a–c respectively. When the reaction time lasted (during addition), from 30 to 45, nanoparticles with bigger diameter were obtained that is consistent with Oswald ripening.

Influence of solvent on the morphology of the CeO_2 which is synthesized in propylene glycol at 60 W (30 min) with CTAB, SDS and PVP are shown in Fig. 7a–c respectively. Results show that by using CTAB, morphology was changed and CeO_2 nanoparticles with average diameter of 50 nm are achieved. By using

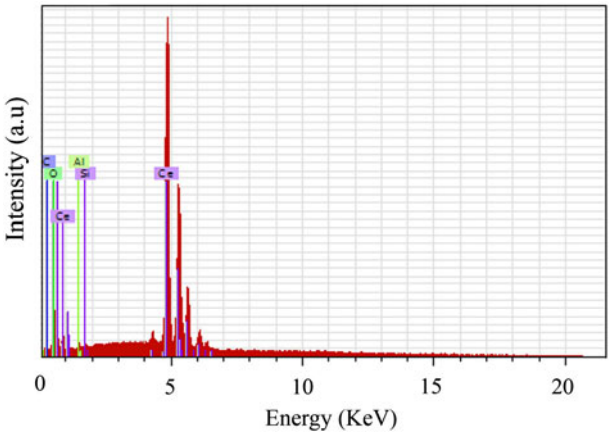

Fig. 8 EDX spectrum of the CeO_2 nanoparticles

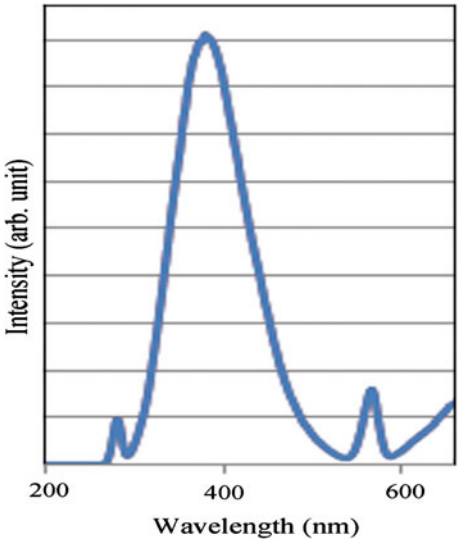

Fig. 9 PL spectrum of the CeO_2 nanoparticles

PVP some agglomeration in particle size observed and slate-like nanostructures were synthesized.

Chemical purity of the CeO_2 nanoparticles was tested by EDX. Figure 8 shows the typical EDX pattern of the sample prepared at 75 W which besides the peaks of Ce and O also peaks of Al and Si related to surface conductor thin film there were no other peaks for impurities.

Photoluminescence (PL) measurement of CeO_2 was carried out at room temperature that is illustrated in Fig. 9. The PL spectrum was consisted of a strong peak at 381 nm that can be ascribed to a high level transition in CeO_2 semiconductor crystallites. It has been reported that this kind of band edge

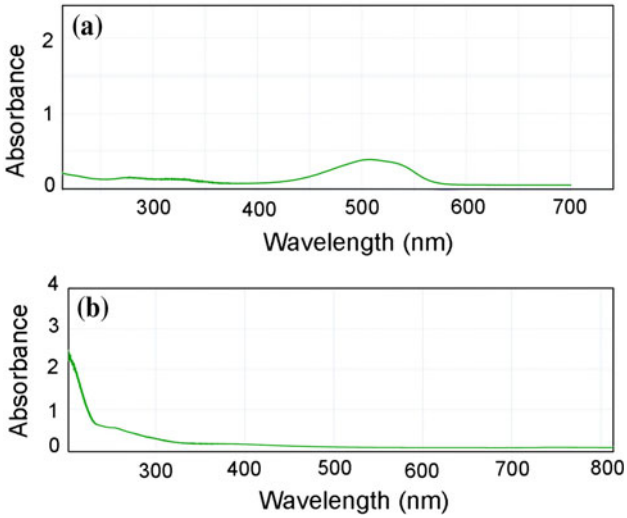

Fig. 10 Absorption spectra under UV light **a** pure MeO solution and **b** MeO in the presence of CeO_2 nanoparticles

luminescence arises from the recombination of excitons and/or shallowly trapped electron–hole pairs [14].

The photocatalytic activity of the nanoparticles was evaluated by monitoring the degradation of MeO in an aqueous solution, under irradiation with UV light. The changes in the concentration of MeO are illustrated in Fig. 10. As time increased, more and more MeO were adsorbed on the nanoparticles catalyst, until the absorption peak ($\lambda = 510$ nm) vanish. The MeO concentration decreased rapidly with increasing UV-irradiation time, and the peak almost disappeared after 60 min. A comparison between TiO_2 (50 nm) and as-synthesized CeO_2 has been done. By using TiO_2 the peak almost disappeared after 40 min [19–21].

Conclusions

CeO_2 nanoparticles were synthesized via a surfactant-free sonochemical reaction at room temperature in water solution. Nanoparticles were characterized using XRD, SEM, EDX and PL techniques. The effect of different parameters such as reaction time, temperature, precursor, surfactant and power on the morphology of the products was investigated. It was found that the as-obtained CeO_2 nanoparticles exhibit a strong PL peak at 381 nm at room temperature. The photocatalytic behavior of nanoparticles was evaluated using the degradation of a MeO aqueous solution under ultraviolet light irradiation. The results show that nanoparticles are favorable materials with excellent performance in photocatalytic applications.

Acknowledgments Authors are grateful to the council of Iran National Science Foundation and University of Kashan for supporting this work by Grant No (159271/80).

References

1. A. Saadat-Monfared, M. Mohseni, and M. Hashemi Tabatabaei (2012). *Colloid. Surf. A* **408**, 64.
2. C. Hu, Z. Zhang, H. Liu, P. Gao, and Z. Lin Wang (2006). *Nanotechnology* **17**, 5983.
3. C. Sun, H. Li, H. Zhang, Z. Wang, and L. Chen (2005). *Nanotechnology* **16**, 1454.
4. P. Dutta, S. Pal, and M. S. Seehra (2006). *Chem. Mater.* **18**, 5144.
5. F. Zhang, P. Wang, J. Koberstein, S. Khalid, and Siu-Wai. Chan (2004). *Surf. Sci.* **563**, 74.
6. T. Masui, H. Hirai, N. Imanaka, G. Adachi, T. Sakata, and H. Mori (2002). *J. Mater. Sci. Lett* **21**, 489.
7. D. Zhang, H. Fu, L. Shi, C. Pan, Q. Li, Y. Chu, and W. Yu (2007). *Inorg. Chem.* **46**, 2446.
8. A. I. Y. Tok, F. Y. C. Boey, Z. Dong, and X. L. Sun (2007). *J. Mater. Process. Tech.* **190**, 217.
9. Z. Wu, J. Zhang, R. E. Benfield, Y. Ding, D. Grandjean, Z. Zhang, and X. Ju (2002). *J. Phys. Chem. B* **106**, 4569.
10. C. Kitiwiang and S. Phanichphant (2009). *J. Microsc. Soc. Thailand* **23**, (1), 83.
11. M. Salavati-Niasari, G. Hosseinzadeh, and F. Davar (2011). *J. Alloys. Compd.* **509**, 134.
12. M. Esmaeili-Zare, M. Salavati-Niasari, and A. Sobhani (2012). *Ultrason. Sonochem.* **19**, 1079.
13. G. Kianpour, M. Salavati-Niasari, and H. Emadi (2012). *Ultrason. Sonochem.* **20**, (1), 418.
14. M. Salavati-Niasari, D. Ghanbari, and M. R. Loghman-Estarki (2012). *Polyhedron* **35**, 149.
15. T. J. Mason, J. P. Lorimer, and D. M. Bates (1992). *Ultrasonics* **30**, 40.
16. Y. J. Chen, L. W. Huang, and T. S. Shih (2003). *Mater. Trans.* **44**, 327.
17. S. Popinet and S. Zaleski (2002). *J. Fluid Mech.* **464**, 137.
18. H.R. Momenian, S. Gholamrezaei, M. Salavati-Niasari, B. Pedram, F. Mozaffar, D.,and Ghanbari (2013) *J. Clust. Sci*., DOI 10.1007/s10876-013-0595-y.
19. S. R. Shirsath, D. V. Pinjari, P. R. Gogate, S. H. Sonawane, and A. B. Pandit (2013). *Ultrason. Sonochem.* **20**, 277.
20. D. V. Pinjari and A. B. Pandit (2011). *Ultrason. Sonochem.* **18**, 1118.
21. K. Prasad, D. V. Pinjari, A. B. Pandit, and S. T. Mhaske (2010). *Ultrason. Sonochem.* **17**, 697.